Original Article
OBESITY BIOLOGY AND INTEGRATED PHYSIOLOGY

Obesity

Positive Interaction Between Prebiotics and Thiazolidinedione Treatment on Adiposity in Diet-Induced Obese Mice

Maud Alligier[1], Evelyne M. Dewulf[1], Nuria Salazar[1], Aline Mairal[2], Audrey M. Neyrinck[1], Patrice D. Cani[1,3], Dominique Langin[2,4] and Nathalie M. Delzenne[1]

Objectives: To investigate whether inulin-type fructan (ITF) prebiotics could counteract the thiazolidinedione (TZD, PPARγ activator) induced-fat mass gain, without affecting its beneficial effect on glucose homeostasis, in high-fat (HF) diet fed mice.

Methods: Male C57bl6/J mice were fed a HF diet alone or supplemented with ITF prebiotics (0.2 g/day $\times$ mouse) or TZD (30 mg pioglitazone (PIO)/kg body weight $\times$ day) or both during 4 weeks. An insulin tolerance test was performed after 3 weeks of treatment.

Results: As expected, PIO improved glucose homeostasis and increased adiponectinaemia. Furthermore, it induced an over-expression of several PPARγ target genes in white adipose tissues. ITF prebiotics modulated the PIO-induced PPARγ activation in a tissue-dependent manner. The co-treatment with ITF prebiotics and PIO maintained the beneficial impact of TZD on glucose homeostasis and adiponectinaemia. Moreover, the combination of both treatments reduced fat mass accumulation, circulating lipids and hepatic triglyceride content, suggesting an overall improvement of metabolism. Finally, the co-treatment favored induction of white-to-brown fat conversion in subcutaneous adipose tissue, thereby leading to the development of brite adipocytes that could increase the oxidative capacity of the tissue.

Conclusions: ITF prebiotics decrease adiposity and improve the metabolic response in HF fed mice treated with TZD.

Obesity (2014) **22**, 1653–1661. doi:10.1002/oby.20733

Introduction

Obesity, characterized by an excessive accumulation of fat mass, mainly results from an imbalance between energy intake and expenditure. Obesity is associated with numerous metabolic disorders including impairment of glucose and lipid homeostasis and alteration of gut microbiota composition (1-4). In this context, nutritional tools are used to positively modulate gut microbiota and improve host metabolism. Among these, inulin-type fructans (ITF), which are non-digestible fermentable carbohydrates, have shown promising prospects in the management of obesity and related disorders (5). Indeed, in obese rodents, they selectively and profoundly change gut microbiota composition, leading to an improvement of the metabolic alterations related to obesity (6-9). These ITF prebiotics are able to counteract the important fat mass accumulation observed in high-fat (HF) diet fed mice (7,10,11). The excessive adiposity induced by HF diet is known to be related to the activation of the peroxisome proliferator-activated receptor gamma (PPARγ) in subcutaneous adipose tissue (SAT) (11), PPARγ being a master regulator of adipocyte differentiation (12). We have shown that HF diet leads to an increased adipocyte size in SAT, related to an over-expression of several PPARγ target genes being implicated in fatty acid metabolism. Interestingly, ITF prebiotics can counteract these

[1] Nutrition and Metabolism Research Group, LDRI, Université catholique de Louvain, Brussels, Belgium. Correspondence: Nathalie M. Delzenne (nathalie.delzenne@uclouvain.be) [2] INSERM, UMR1048, Obesity Research Laboratory, Institute of Metabolic and Cardiovascular Diseases, University of Toulouse, Paul Sabatier University, Toulouse, France [3] WELBIO, Walloon Excellence in Life sciences and BIOtechnology, Université catholique de Louvain, Brussels, Belgium [4] Department of Clinical Biochemistry, Toulouse University Hospitals, Toulouse, France

Funding agencies: MA is the recipient of a grant of the SFD (Société Francophone du Diabète). NS is the recipient of a postdoctoral fellowship from the Spanish Ministry of Education, Culture and Sports. PDC is a Research Associate from the FRS-FNRS Belgium and a recipient of ERC Starting grant 2013 (ENIGMO). This project was supported by FNRS grant (no. 1.5121.12 to NMD), ANR grant mirBAT (to DL) and European FP7 Collaborative Project DIABAT (HEALTH-F2-2011-278373 to DL).

Disclosure: The authors have no competing interest.

Author contributions: EMD and NMD designed the protocol. EMD and NS carried out the *in vivo* experiments. MA, EMD, and NS collected the data. MA, EMD, and AM performed histological, biochemical, and molecular analyses. MA, EMD, AMN, PDC, DL, and NMD interpreted the data. MA, EMD, and ND wrote the paper. All authors read and approved the final manuscript.

Maud Alligier and Evelyne M. Dewulf contributed equally to this work

Received: 11 October 2013; **Accepted:** 23 February 2014; **Published online 19 April 2014. doi:10.1002/oby.20733**

effects, suggesting a potential impact of the prebiotic treatment on PPARγ activity (11).

Thiazolidinediones (TZD) are well-known PPARγ activators which are used as anti-diabetic agents in humans (13). TZD are "adipose remodeling factors" that increase the number of small, newly differentiated, insulin-responsive adipocytes in SAT, thus improving lipid storage in this tissue. This reduces visceral fat development and ectopic lipid deposition, thus decreasing the lipotoxicity and the related insulin-resistance in other organs. Moreover, they modulate the production/secretion of some adipokines implicated in insulin signaling, thereby reinforcing their beneficial impact on glucose homeostasis (14,15). However, TZD also induce fat mass accumulation, a main side effect (13,16,17).

The aim of our study was to investigate whether ITF prebiotics were able to counteract the side effect of PPARγ activation on adiposity without changing the insulin-sensitizing potency of the PPARγ agonist. Therefore, we used the TZD pioglitazone (PIO) as a pharmacological tool to modulate PPARγ activity in a model of HF diet-induced obesity.

Methods

Animals

Ten-week-old male C57bl6/J mice (Charles River, Brussels, Belgium) were separated into five groups: the CT group received a control diet (AO4, SAFE, Villemoison-sur-Orge, France), the HF group received a HF diet (D12492, Research Diets, New Brunswick, NJ), the HF-ITF group received the HF diet and 0.2 g/day×mouse of ITF prebiotic in water (oligofructose from Orafti, Oreye, Belgium), the HF-PIO group received the HF diet supplemented with 30 mg/kg body weight×day of PIO (Actos®, kindly provided by Takeda Pharmaceuticals BeNeLux, Brussels, Belgium), and the HF-PIO-ITF group received the HF diet supplemented with PIO and ITF prebiotics. Mice were treated for 4 weeks. Food intake, taking into account spillage, and water consumption were recorded twice a week. Total energy consumption was calculated based upon diet's energy content and ITF supplementation in water (2 cages/group). Body composition was assessed by using a 7.5-MHz TD-NMR (LF50 minispec; Bruker, Rheinstetten, Germany).

The experiment was approved by the local committee and the housing conditions were as specified by the Belgian Law of May 29, 2013 on the protection of laboratory animals (agreement no. LA 1230314).

Insulin tolerance test

After 3 weeks of treatment, 6 h-fasted mice received an intraperitoneal (i.p.) injection of insulin (1 mU/g body weight). Blood glucose was determined with a glucose meter (Roche Diagnostic, Meylan, France).

Blood and tissue samples

At the end of the experiment, 6 h-fasted mice were anesthetized with isoflurane (ForeneH, Abbott, Queenborough, Kent, England). Blood from cava vein was collected, centrifuged (3 min, 13,000*g*) and plasma was stored at −80°C. Then mice were then killed by cervical dislocation. Liver, caecum, white adipose tissues [subcutaneous (SAT) and visceral (VAT)], brown adipose tissue (BAT), and muscles (*gastrocnemius* and *soleus*) were collected, weighed, and frozen in liquid N_2 or kept in formaldehyde solution for histological analysis.

Adipose tissue morphometry

The mean adipocyte size was estimated on paraffin-embedded hematoxylin-stained eosin-counterstained sections of SAT and VAT. The number of adipocytes per microscopic field (density) was determined as previously described by Dewulf et al. (11).

Blood biochemical analysis

Systemic blood glucose concentration was determined using a glucose meter (Roche Diagnostic, Meylan, France). Plasma free fatty acids, triglycerides, and glycerol were determined by enzymatic reactions and spectrophotometric detection of reaction end-products (Randox Laboratories Ltd., Crumlin, United Kingdom; Diasys Diagnostic and Systems, Holzheim, Germany; Sigma-Aldrich, Saint Louis, MO, respectively). Plasma insulin and adiponectin concentrations were determined using ELISA kits (ALPCO Diagnostics, Salem, NH; R&D Systems, Inc., Minneapolis, MN, respectively), following the manufacturer's instructions.

Real-time quantitative PCR

Total RNA was isolated from tissues using the TriPure isolation reagent kit (Roche Diagnostics Belgium, Vilvoorde). Quantification and integrity analysis of total RNA was assessed with an Agilent 2100 Bioanalyzer (Agilent RNA 6000 Nano Kit, Agilent, Santa Clara, CA). cDNA was prepared using the Kit Reverse Transcription System (Promega, Leiden, The Netherlands). Real-time quantitative polymerase chain reactions (RT-qPCR) were performed with the StepOne Plus real time PCR system and software (Applied Biosystems, Den Ijssel, The Netherlands) using SYBR-Green (Eurogentec, Verviers, Belgium or Applied Biosystems) for detection. Ribosomal protein L19 (RPL19) RNA was chosen as housekeeping gene. All primers are available upon request. All samples were run in duplicate in a single 96-well reaction plate and data were analyzed according to the $2^{-\Delta CT}$ method.

UCP1 immunohistochemistry

We evaluated the UCP1 (Uncoupling protein 1) immunoreactivity on paraffin-embedded SAT sections. These sections were firstly incubated with a primary rabbit anti-mouse UCP1 polyclonal antibody (1:150, Abcam, Cambridge, UK) and secondly with the Peroxidase Labeled Polymer solution which contained the secondary anti-rabbit antibody, provided by the immunochemistry kit (Dako, Glostrup, Denmark). Finally, peroxidase activity was revealed with diaminobenzidine (DAB). For evaluation of UCP1 protein level staining, each section was analyzed in duplicate in a double-blind manner by two different investigators and a score was assigned according to the levels of UCP1 presence.

UCP1 Western blotting

Adipose tissues were homogenized in a RIPA buffer, centrifuged for 25 min at 15,000*g* and supernatants were stored at −80°C. The concentration of the protein preparation was determined using the

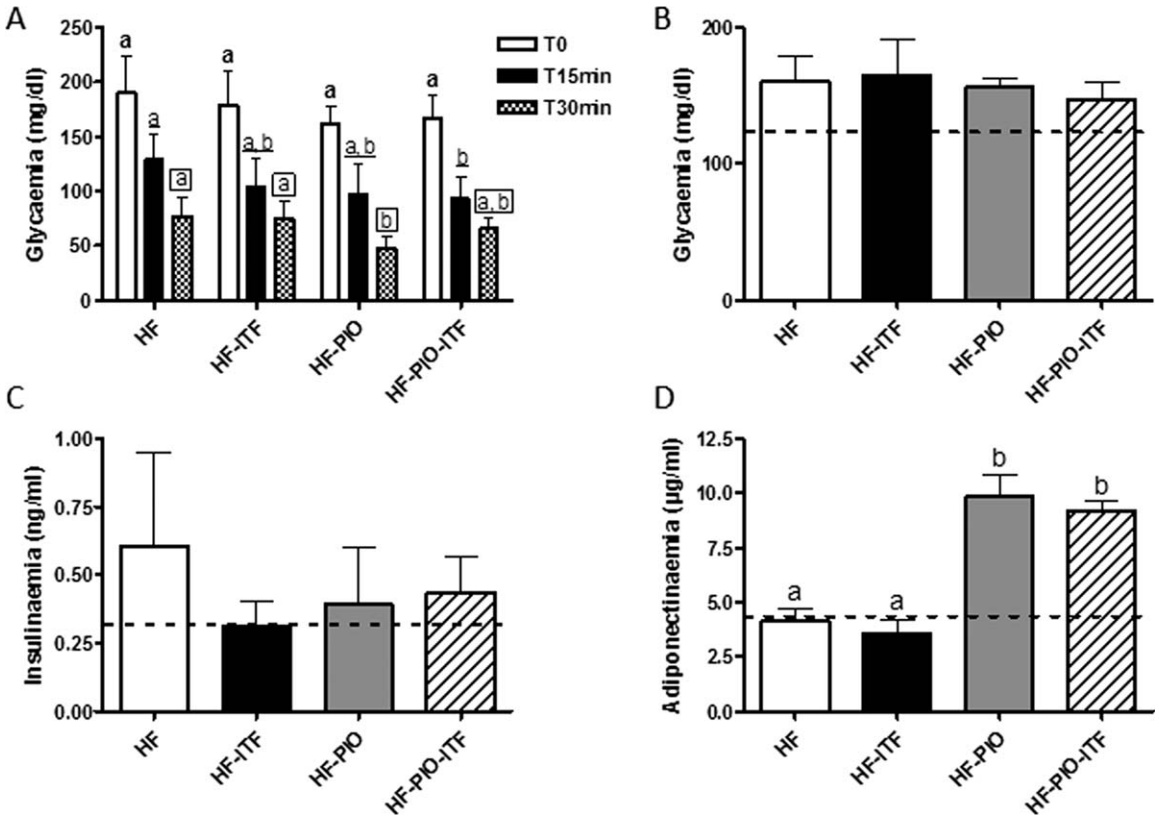

Figure 1 Glucose homeostasis in mice fed a HF diet alone or supplemented with ITF and/or PIO after 4 weeks of treatment (n = 7 or 8/group). **A**: Insulin tolerance test: glucose levels 0, 15, and 30 min after insulin injection. One-way ANOVA statistical analysis performed at each time point (bold letters at T0, underlined letters at T15 min and circled letters at T30 min); (**B–D**) Fasting glycaemia, insulinaemia, and adiponectin levels. The dotted line represents the mean value of CT mice. Data are mean ± SD. Data with different superscript letters are significantly different at $P < 0.05$, according to the *post hoc* ANOVA statistical analysis.

Bradford method. Given to the large amount of protein required for this analysis and the limited available tissue amount, the Western blotting analysis was not performed in all mice, but at least five mice per group were used. About 45 µg of solubilized proteins were run on a Criterion TGX Stain-Free 4-20% precast gel (Bio-Rad, Hercules, CA). Stain-free imaging was performed according to the manufacturer's instructions, with a 1-min stain activation time to visualize total proteins. Proteins were then transferred onto nitrocellulose membrane, using a Turbo Blot transfer unit (Bio-Rad). Membranes were blocked in 5% skim milk/Tris-buffered saline (TBS)/0.2% Tween 20 (1 h, at 4°C) and incubated overnight at 4°C with the primary antibody UCP1 (cat no. ab10983, Abcam Inc., Cambridge, MA) diluted 1:1,000. Horseradish peroxidase (HRP)-linked anti-rabbit secondary antibody (Cell Signaling Technology Inc., Beverly, MA) diluted 1:10,000, was incubated at 4°C for 1 h. Chemiluminescence from the reaction of HRP-linked secondary antibody and Clarity solution was captured digitally using a ChemiDoc MP imager (Bio-Rad). All images were analyzed using Image Lab 4.0.1 software (Bio-Rad). UCP1 signal was normalized to total proteins for each lane.

Statistical analysis

Results are presented as mean ± SD. The dotted line on the graphs represents the mean value of CT mice. The number of concerned mice for each experiment is notified in each legend. To note, that one mouse was dead during the NMR experiment and another was excluded by a specific statistical analysis, due to abnormal and discordant data (technical problem during the procedure). Statistical significance of difference between groups fed the HF diet was assessed by one-way analysis of variance (ANOVA) followed by *post hoc* Tukey's multiple comparison tests in Graph-Pad Prism (version 5.00 for Windows, GraphPad Software, San Diego, CA). Data with different superscript letters are significantly different ($P < 0.05$) according to the *post hoc* ANOVA statistical analysis.

Results

ITF prebiotics maintain the beneficial impact of pioglitazone on glucose homeostasis

HF diet slightly disturbed glucose homeostasis by increasing fasting glycaemia and insulinaemia as compared to CT mice (Figure 1B and C). Furthermore, during insulin tolerance test (ITT), the fall of glycaemia 15 min after insulin injection was less pronounced in HF fed mice than in the CT group (54% of glycaemia at T0 in CT group versus 70% in HF group). PIO improved the response to insulin during ITT, with a significantly lower glycaemia 30 min following insulin injection as compared to HF fed mice (Figure 1A), and

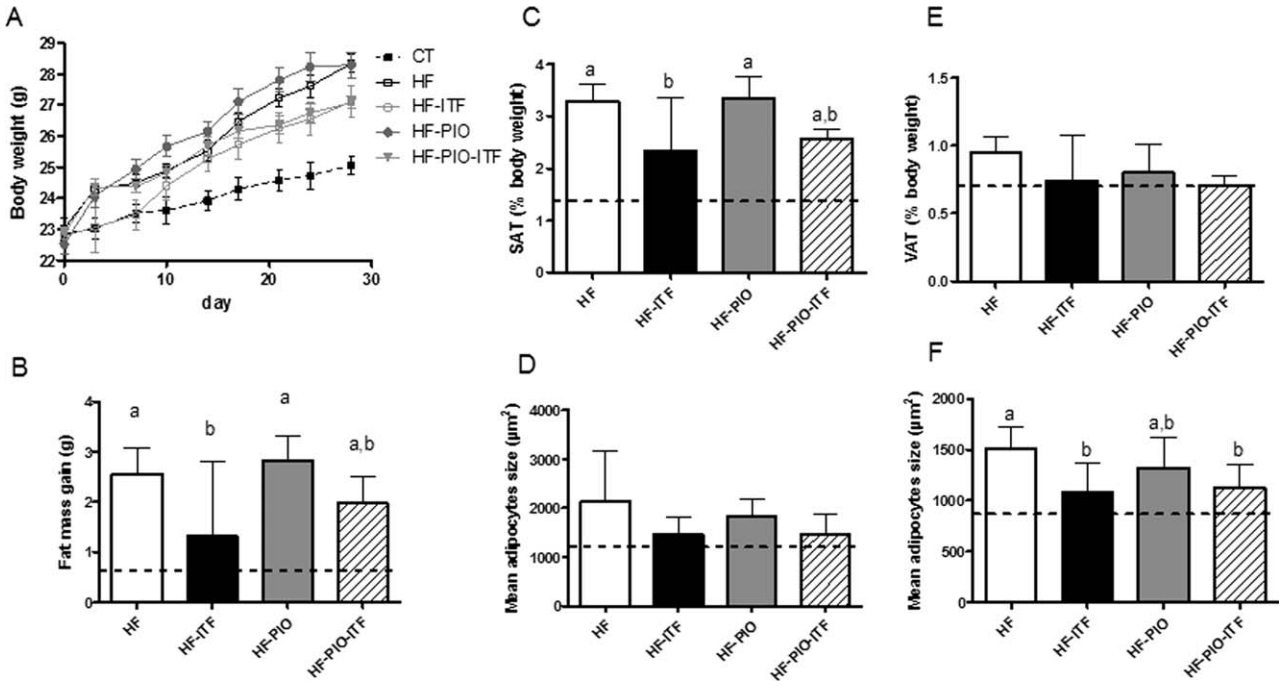

Figure 2 Body composition in mice fed a HF diet alone or supplemented with ITF and/or PIO after 4 weeks of treatment (n = 7 or 8/group). **A**: Body weight. **B**: Fat mass gain. **C**: Subcutaneous adipose tissue (SAT) weight. **D**: Visceral adipose tissue (VAT) weight. **E**: Adipocytes size in SAT. **F**: Adipocytes size in VAT. The dotted line represents the mean value of CT mice. Data are mean ± SD. Data with different superscript letters are significantly different at $P < 0.05$, according to the *post hoc* ANOVA statistical analysis.

tended to decrease insulinaemia (Figure 1C). The administration of ITF prebiotics to PIO-treated mice preserved the beneficial effects of TZD on glucose homeostasis. As expected, PIO induced a huge increase in plasma adiponectin level, which was maintained with the prebiotic supplementation (Figure 1D).

ITF prebiotics decrease fat mass in pioglitazone-treated animals

Total energy consumption was slightly increased upon PIO and decreased in prebiotic treated mice but these differences were extremely low in terms of consumed energy (HF: 13.02, HF-ITF: 12.35, HF-PIO: 13.77, HF-PIO-ITF: 12.14 kcal/day×mouse). The body weight evolution and the fat mass gain are shown in Figure 2A and B. As expected, the body weight gain expressed in grams (or in percentage of initial body weight) was increased with the HF diet alone in the same way as fat mass within 4 weeks, and PIO tended to reinforce the body weight gain (HF: 5.8 g (25%)^{ab}, HF-ITF: 4.8g (22%)^{a}, HF-PIO: 6.6g (26%)^{b}, HF-PIO-ITF: 4.8g (20%)^{a}; data with different superscript letters are significantly different at $P < 0.05$, according to the *post hoc* ANOVA statistical analysis). The combination of PIO and ITF prebiotics significantly decreased body weight gain as compared to treatment with PIO alone. However, PIO did not change significantly adipose tissues weight, nor adipocyte size in SAT and VAT (Figure 2C–F). ITF prebiotics lessened fat mass development driven by the HF diet, mainly with a significant decrease in total and subcutaneous fat mass (Figure 2B and C). Interestingly, they also decreased mean adipocyte size, but this effect was only significant in VAT (Figure 2F).

Pioglitazone induces PPARγ activation in white adipose tissues and prebiotics modulate this activity in a tissue-dependent manner

PIO induced an over-expression of several PPARγ target genes (aP2: activating protein 2, CD36: cluster of differentiation 36 and adiponectin) in SAT and VAT but this PPARγ activation was much more pronounced in VAT (Figure 3). ITF prebiotics alone did not modify the expression of these genes in both tissues and did not counteract the PIO induced-PPARγ activation in SAT. In contrast, the prebiotic treatment completely blunted the effect of PIO on PPARγ target genes expression in VAT, suggesting a tissue-dependent effect of ITF prebiotics.

Co-treatment with ITF prebiotics and pioglitazone modulates lipid metabolism

Each treatment alone had no significant impact on hepatic and systemic triglycerides (TG), free fatty acids (FFA), or glycerol whereas the co-treatment significantly decreased all these parameters as compared to HF fed mice (Figure 4). However, PIO and/or ITF prebiotics had no significant impact on the expression levels of genes implicated in fatty acid oxidation (PPARα, CPT1a: carnitine palmitoyl transferase 1, Hadh: 3-hydroxyacyl-CoA dehydrogenase), lipogenesis (FAS: fatty acid synthase) or TG export (MTTP: microsomal triglycerides transfer protein) (Table 1).

Finally, PIO did not significantly change muscle mass whereas the PIO-ITF co-treatment increased soleus muscle mass as compared to

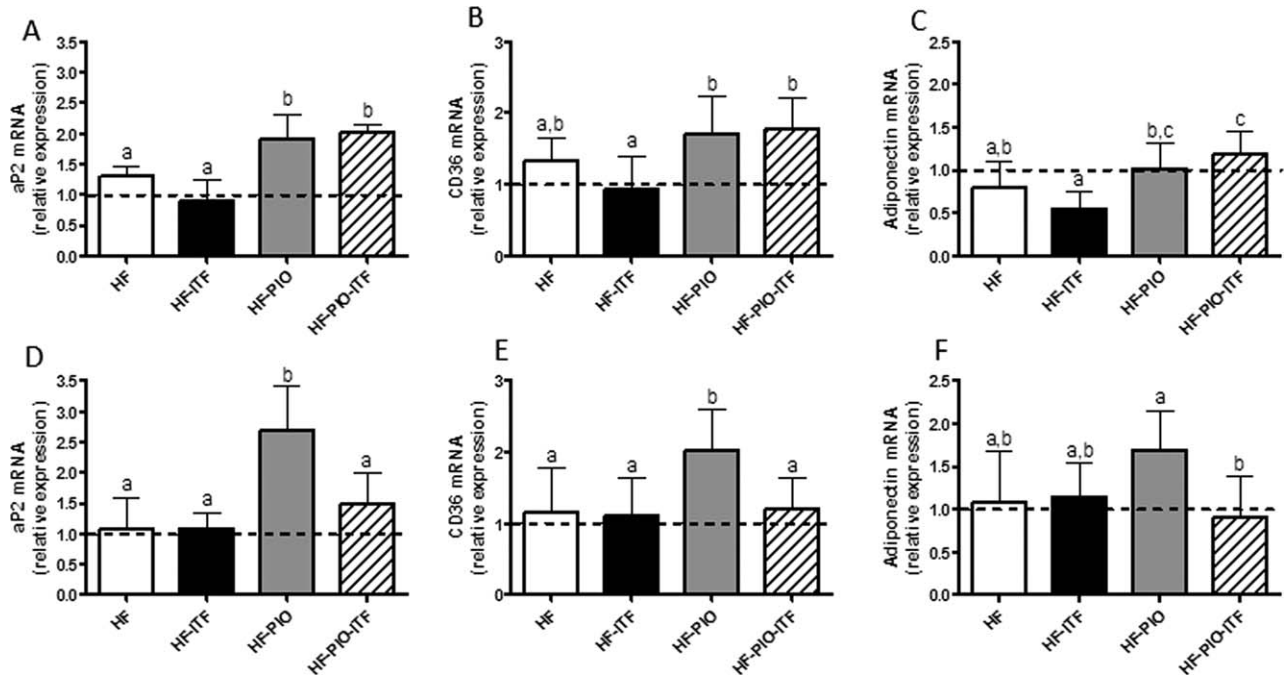

Figure 3 Expression of PPARγ target genes in subcutaneous adipose tissue (**A–C**) and visceral adipose tissue (**D–F**) of mice fed a HF diet alone or supplemented with ITF and/or PIO after 4 weeks of treatment (n = 7 or 8/group). aP2: Activating protein 2; CD36: Cluster of differentiation 36. The dotted line represents the mean value of CT mice that was set at 1. Data are mean ± SD. Data with different superscript letters are significantly different at $P < 0.05$, according to the *post hoc* ANOVA statistical analysis.

PIO treatment alone (Figure 5). We observed no significant effect of the different treatments on the expression of two oxidative genes (PGC1α: PPARγ coactivator 1-alpha and CPT1b) in muscles (Table 1).

ITF prebiotics maintain the modulation of brown adipose tissue activity observed upon pioglitazone treatment

PIO induced an important accumulation of BAT mass whereas the HF diet had no impact on this tissue as compared to CT mice (Figure 6A). Furthermore, we observed an over-expression of aP2 and UCP1 in BAT of HF-PIO fed mice, suggesting an activation of PPARγ (Figure 6B and C). ITF prebiotics did not change BAT weight but lessened the PIO-induced BAT development without modifying the expression of PPARγ target genes. In contrast, PIO did not modulate the expression of genes of fatty acid oxidation and mitochondrial oxidative capacity (PPARα, CPT1b, and PGC1α) whereas the co-administration of PIO and ITF led to an over-expression of PPARα and tended to increase CPT1b and PGC1α mRNAs as compared to PIO alone (Figure 6D–F).

ITF prebiotics and pioglitazone combination may induce white-to-brown fat conversion in subcutaneous adipose tissue

It has been already demonstrated that PPARγ activation can induce a white-to-brown fat conversion phenomenon in rodent SAT (18-21). Briefly, this process requires expression of PRD1-BF1-RIZ1 homologous domain containing-16 (PRDM16) and PGC1α, two master regulators of brown adipocyte differentiation, and allows the formation of brite (from "brown in white") adipocytes (22-24). These brite adipocytes exhibit characteristics of both white and brown adipocytes and possess a high oxidative capacity, due to the presence of UCP1 protein (25).

PIO and ITF co-treatment significantly increased PRDM16 mRNA, as compared to HF fed mice, while PIO alone did not. Moreover, PGC1α expression tended to be up-regulated by the co-treatment whereas the other conditions did not affect this factor (Figure 7A). To estimate the presence of brite adipocytes in SAT, we tried to quantify UCP1 protein level by Western blotting. Although the result was heterogeneous, ITF and PIO combination seemed to increase UCP1 protein expression in 4 of 8 mice whereas each treatment alone had no clear effect (Figure 7B). We also performed an immunohistochemistry analysis of UCP1 to visualize the protein in our samples. Although this analysis remains qualitative, the result seemed to confirm the Western blotting analysis, since a slight increase of the UCP1 level staining was also observed in the co-treated group (Figure 7C), mainly due to the presence of staining foci (as depicted in the picture in Figure 7D).

Discussion

TZD, such as PIO, are PPARγ activators used as anti-diabetic agents. However, they induce several side effects such as cardiovascular disease or renal injury and also body weight gain in rodents and humans. This last side effect is a concern in the management of diabetes in already obese individuals (13). The aim of our study was

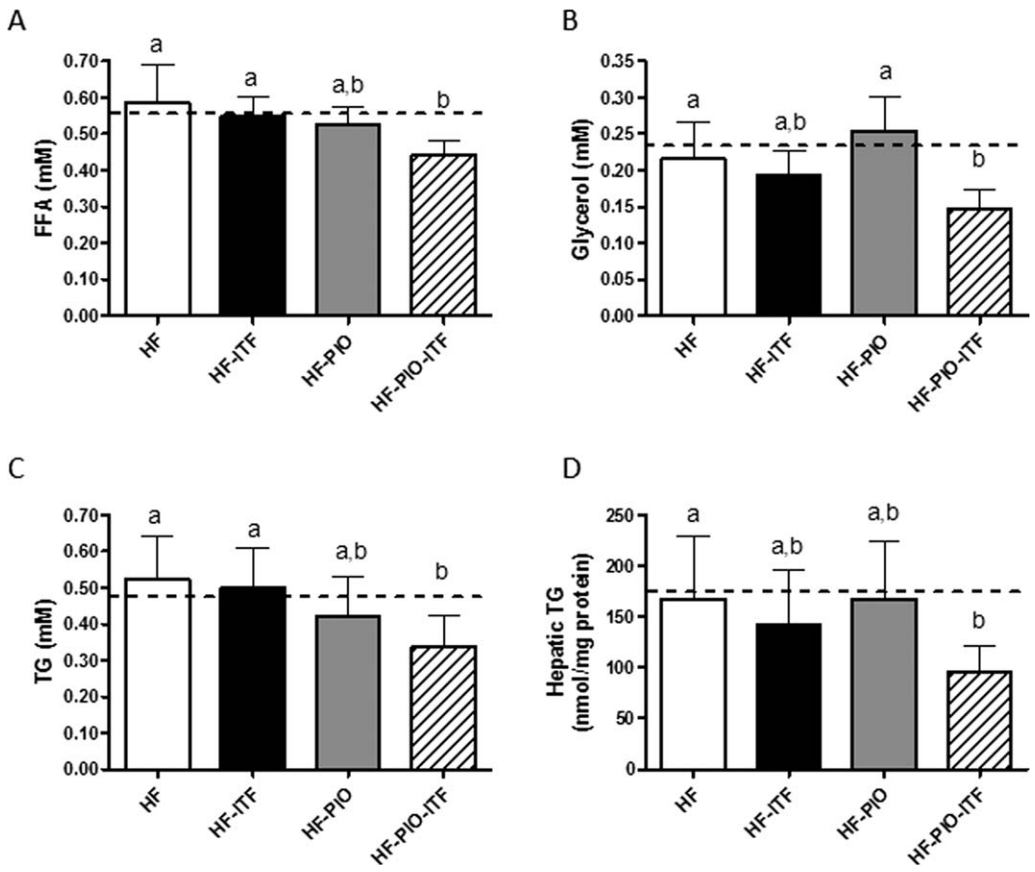

Figure 4 Plasma (**A, B, C**) and hepatic (**D**) parameters of lipid metabolism in mice fed a HF diet alone or supplemented with ITF and/or PIO after 4 weeks of treatment ($n = 7$ or 8/group). The dotted line represents the mean value of CT mice. Data are mean ± SD. Data with different superscript letters are significantly different at $P < 0.05$, according to the *post hoc* ANOVA statistical analysis. TG: triglycerides; FFA: free fatty acids.

TABLE 1 Expression of genes in liver, gastrocnemius, and soleus muscles

Relative expression	HF	HF-ITF	HF-PIO	HF-PIO-ITF
Liver				
PPARα mRNA	1.10 ± 0.12	1.09 ± 0.26	0.95 ± 0.10	0.99 ± 0.18
CPT1a mRNA	0.97 ± 0.30	1.02 ± 0.34	0.96 ± 0.37	0.64 ± 0.15
Hadh mRNA	1.21 ± 0.25	1.30 ± 0.30	1.41 ± 0.17	1.09 ± 0.16
FAS mRNA	0.68 ± 0.18	0.73 ± 0.22	0.80 ± 0.16	0.79 ± 0.20
MTTP mRNA	0.81 ± 0.40	0.75 ± 0.33	0.54 ± 0.27	0.44 ± 0.13
Gastrocnemius				
PGC1α mRNA	1.05 ± 0.17	1.09 ± 0.34	1.07 ± 0.36	0.79 ± 0.28
CPT1b mRNA	1.09 ± 0.26	1.19 ± 0.35	1.46 ± 0.45	0.85 ± 0.53
Soleus				
PGC1α mRNA	0.96 ± 0.34	1.05 ± 0.51	1.27 ± 0.72	0.75 ± 0.40
CPT1b mRNA	1.20 ± 0.42	1.63 ± 0.35	1.25 ± 0.41	1.31 ± 0.40

Data are mean ± SD ($n = 7$ or 8/group). Mean value obtained in the CT group was set at 1. CPT1: carnitine palmitoyl transferase 1; FAS: fatty acid synthase; Hadh: 3-hydroxyacyl-CoA dehydrogenase; MTTP: microsomal triglycerides transfer protein; PGC1α: peroxisome proliferator-activated receptor gamma coactivator 1-alpha; PPARα: peroxisome proliferator-activated receptor alpha.

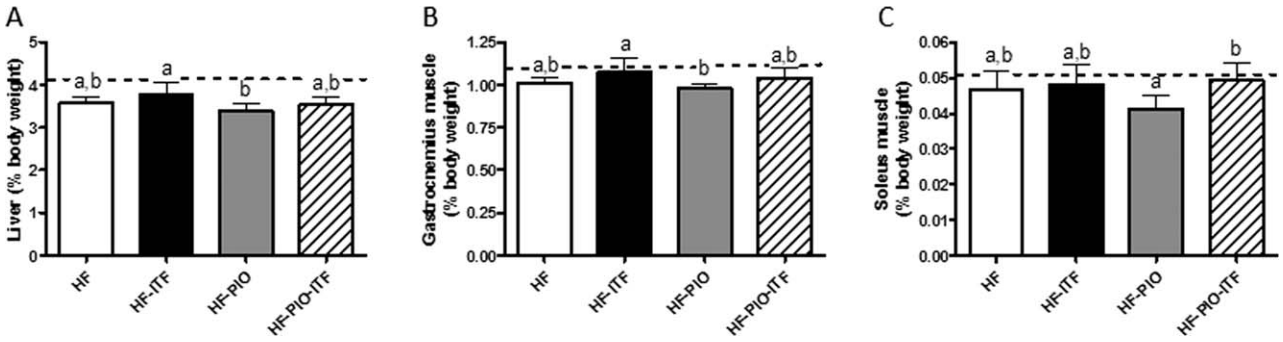

Figure 5 Liver (**A**), gastrocnemius muscle (**B**), and soleus muscle (**C**) weights in mice fed a HF diet alone or supplemented with ITF and/or PIO after 4 weeks of treatment ($n = 7$ or 8/group). The dotted line represents the mean value of CT mice. Data are mean ± SD. Data with different superscript letters are significantly different at $P < 0.05$, according to the *post hoc* ANOVA statistical analysis.

to focus on TZD-induced adiposity gain, and investigate whether ITF prebiotics were able to reduce it without preventing the insulin-sensitizing property of TZD in a model of diet-induced obesity.

Concerning glucose homeostasis, PIO-ITF co-treatment was the most efficient to decrease glucose levels 15 min after an i.p. challenge of insulin (ITT). As expected, PIO markedly increased circulating adiponectin levels, an adipokine that participates in the insulin-sensitizing effect of TZD (14,15) and the co-treatment maintained this increase.

PIO tended to increase the HF diet-induced body weight gain without affecting SAT weight or adipocyte size. This lack of TZD impact on adiposity in HF fed mice has been previously described (26,27). Interestingly, ITF prebiotics reduced adiposity and tended to decrease subcutaneous adipocyte size. As shown by the expression of several PPARγ target genes, we observed a minor PPARγ activation in SAT upon PIO without additional effect of prebiotics. Conversely, in VAT, ITF prebiotics counteracted the PIO-induced overexpression of aP2, CD36, and adiponectin. Unexpectedly, the impact of both treatments on these mRNAs levels in SAT and VAT did not

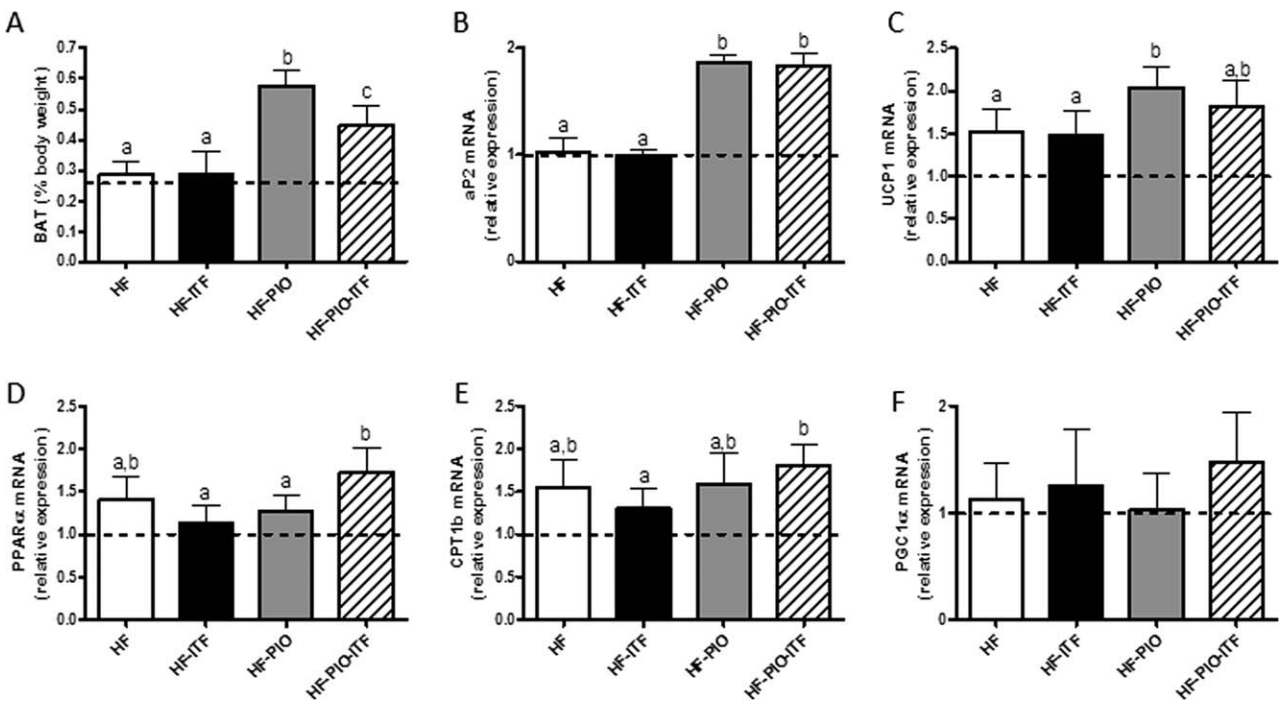

Figure 6 Brown adipose tissue weight (**A**) and gene expression (**B–F**) in mice fed a HF diet alone or supplemented with ITF and/or PIO after 4 weeks of treatment ($n = 7$ or 8/group). The dotted line represents the mean value of CT mice (set at 1 for mRNAs). Data are mean ± SD. Data with different superscript letters are significantly different at $P < 0.05$, according to the *post hoc* ANOVA statistical analysis.

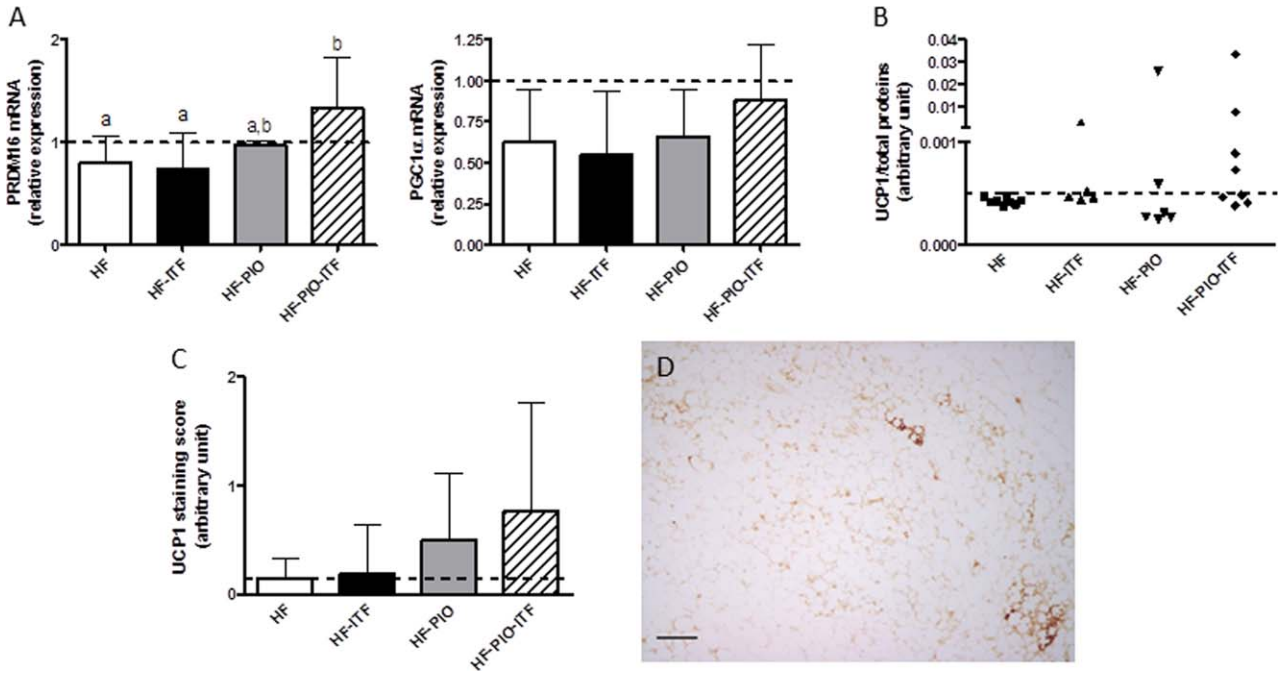

Figure 7 Assessment of white-to-brown fat conversion in SAT of mice fed a HF diet alone or supplemented with ITF and/or PIO after 4 weeks of treatment. **A**: Expression of PRDM16 (PRD1-BF1-RIZ1 homologous domain containing-16) and PGC1α (PPARγ coactivator 1-alpha); (**B**) UCP1 (Uncoupling protein 1) Western blotting (n = 5 or 6/group); (**C**) UCP1 immunohistochemistry: staining score, assigned to each section according to the levels of UCP1 presence (left, n = 7 or 8/group) and histological picture from one HF-PIO-ITF mouse (right, bar = 100 μm). The dotted line represents the mean value of CT mice set at 1. Data are mean ± SD. Data with different superscript letters are significantly different at $P < 0.05$, according to the *post hoc* ANOVA statistical analysis. [Color figure can be viewed in the online issue, which is available at wileyonlinelibrary.com.]

coincide with the observed differences in adipose tissue weight and adipocyte size but highlighted a tissue-specific effect of ITF prebiotics on PPARγ activity.

TZD have been shown to modulate BAT activity by increasing tissue mass and over-expressing UCP1 (28-30). This activation of brown adipocytes may participate in the anti-diabetic properties of TZD by increasing energy dissipation. In our study, we confirmed the important increase of BAT weight in HF-PIO mice as compared to HF fed mice and the over-expression of UCP1. We also observed an increased expression of aP2 which probably reflected the PIO-induced PPARγ activation. ITF prebiotics lessened the BAT expansion induced by PIO, but the tissue weight remained significantly higher than in the HF group. Furthermore, the prebiotic treatment led to an over-expression of PPARα and tended to increase PGC1α mRNA, suggesting a possible increased fatty acid oxidation and mitochondrial oxidative capacity (31-33).

Each treatment alone had no significant effect on lipid metabolism but the co-administration of PIO and ITF prebiotics significantly decreased plasma TG, FFA and glycerol, and hepatic TG content. The effect of TZD and ITF on glycerol, FFA, and plasma triglyceride let us suppose that the combination of both treatments may be beneficial, by limiting the flux of fatty acids issued from lipolysis in the systemic circulation, and through the decrease of a marker of cardiovascular risk (triglyceridemia). Those interesting data only open the door to further analysis of the relevance of those effects in other animal models and in humans.

Therefore, one question remained: what was the metabolic fate of lipids from mice co-treated with ITF prebiotics and PIO? The decrease in fasting FFA and glycerol suggests a possible inhibition of adipose tissue lipolysis. Moreover, lipids were less accumulated in white and brown adipose tissues. In addition, the expression of genes involved in fatty acid oxidation revealed a similar oxidative capacity in muscles and liver. The decrease in plasma TG and hepatic TG content may originate from changes in lipid metabolism in other tissues than liver (e.g., adipose tissues). Additional experiments performed on freshly isolated tissues or using indirect calorimetry would be necessary to assess precisely energy metabolism and substrate oxidation. Otherwise, the minor differences in energy intake observed between PIO and ITF supplemented mice could not explain the changes in lipid profile in HF-PIO-ITF mice.

The conversion of white adipocytes into brite adipocytes could contribute to the increased oxidative capacity of adipose tissue and possibly lessen fat accumulation. It has already been demonstrated that PPARγ activation can induce a brown fat gene program, preferentially in SAT (18-21). This process requires expression of PRDM16 and PGC1α, two master regulators of brown adipocyte differentiation (23,24,34). As ITF prebiotics did not counteract the PIO-induced PPARγ activation in SAT but reduced fat mass, we asked whether these results could be explained by a conversion of adipocyte type and thus increased oxidative capacity upon ITF prebiotic treatment. Therefore, we measured the expression of PRDM16 and PGC1α in SAT. Interestingly, PIO alone did not modify the

expression of both genes whereas the co-treatment led to a significant over-expression of PRDM16 and tended to increase PGC1α mRNA.

To confirm these results, we analyzed UCP1 protein levels, a characteristic marker of brite adipocytes, by Western blotting (25). Although the results did not reach the significance, the combination of ITF prebiotics with PIO seemed to increase UCP1 protein level in half of the mice whereas each treatment alone had only minor effects. These results suggest an increased white-to-brown fat conversion in mice receiving both treatments. Thanks to immunohistochemistry analysis, we observed a slight increase in UCP1 score in the PIO group that seemed further augmented in mice treated with PIO and ITF prebiotics. The variability observed at mRNA and protein levels is probably linked to the heterogeneous spread of brite adipocyte foci in SAT depot as shown in histological section. It would have been preferable to use total SAT pool to assess the co-treatment effect on brite adipocytes appearance. This would have allowed taking into account this heterogeneous distribution of brite adipocytes loci and thus reliably evaluating the phenomenon. Although further mechanistic studies on the process are necessary, we believe that our preliminary results provide some evidences of the presence of brite adipocytes in HF-PIO-ITF mice which could increase the oxidative capacity of SAT, thus participating in fat mass loss.

In conclusion, administration of ITF prebiotics maintained the beneficial impact of PIO treatment on glucose homeostasis. Moreover, prebiotics lessened adiposity and improved overall metabolism in comparison to PIO alone. Although additional *in vivo* studies will be required to examine the other major side effects of TZD treatment, our promising results allow considering the combination of TZD and ITF to treat diabetic patients who are obese, as ITF prebiotics seem to be able to counteract the TZD-induced adiposity. O

Acknowledgments

Authors thank Bouazza Es Saadi and Remi Selleslagh for their technical assistance.

References

1. Ley RE, Backhed F, Turnbaugh P, Lozupone CA, Knight RD, Gordon JI. Obesity alters gut microbial ecology. *Proc Natl Acad Sci USA* 2005;102:11070-11075.
2. Hotamisligil GS. Inflammation and metabolic disorders. *Nature* 2006;444:860-867.
3. Cani PD, Delzenne NM. Interplay between obesity and associated metabolic disorders: new insights into the gut microbiota. *Curr Opin Pharmacol* 2009;9:737-743.
4. Cani PD, Amar J, Iglesias MA, et al. Metabolic endotoxemia initiates obesity and insulin resistance. *Diabetes* 2007;56:1761-1772.
5. Delzenne NM, Neyrinck AM, Backhed F, Cani PD. Targeting gut microbiota in obesity: effects of prebiotics and probiotics. *Nat Rev Endocrinol* 2011;7:639-646.
6. Cani PD, Knauf C, Iglesias MA, Drucker DJ, Delzenne NM, Burcelin R. Improvement of glucose tolerance and hepatic insulin sensitivity by oligofructose requires a functional glucagon-like peptide 1 receptor. *Diabetes* 2006;55:1484-1490.
7. Cani PD, Neyrinck AM, Fava F, et al. Selective increases of bifidobacteria in gut microflora improve high-fat-diet-induced diabetes in mice through a mechanism associated with endotoxaemia. *Diabetologia* 2007;50:2374-2383.
8. Cani PD, Possemiers S, Van de Wiele T, et al. Changes in gut microbiota control inflammation in obese mice through a mechanism involving GLP-2-driven improvement of gut permeability. *Gut* 2009;58:1091-1103.
9. Everard A, Lazarevic V, Derrien M, et al. Responses of gut microbiota and glucose and lipid metabolism to prebiotics in genetic obese and diet-induced leptin-resistant mice. *Diabetes* 2011;60:2775-2786.
10. Delmee E, Cani PD, Gual G, et al. Relation between colonic proglucagon expression and metabolic response to oligofructose in high fat diet-fed mice. *Life Sci* 2006;79:1007-1013.
11. Dewulf EM, Cani PD, Neyrinck AM, et al. Inulin-type fructans with prebiotic properties counteract GPR43 overexpression and PPARgamma-related adipogenesis in the white adipose tissue of high-fat diet-fed mice. *J Nutr Biochem* 2011;22:712-722.
12. Rosen ED, Sarraf P, Troy AE, et al. PPAR gamma is required for the differentiation of adipose tissue in vivo and in vitro. *Mol Cell* 1999;4:611-617.
13. Cariou B, Charbonnel B, Staels B. Thiazolidinediones and PPARgamma agonists: time for a reassessment. *Trends Endocrinol Metab* 2012;23:205-215.
14. Berger JP, Akiyama TE, Meinke PT. PPARs: therapeutic targets for metabolic disease. *Trends Pharmacol Sci* 2005;26:244-251.
15. Combs TP, Wagner JA, Berger J, et al. Induction of adipocyte complement-related protein of 30 kilodaltons by PPARgamma agonists: a potential mechanism of insulin sensitization. *Endocrinology* 2002;143:998-1007.
16. Laplante M, Festuccia WT, Soucy G, et al. Mechanisms of the depot specificity of peroxisome proliferator-activated receptor gamma action on adipose tissue metabolism. *Diabetes* 2006;55:2771-2778.
17. de Souza CJ, Eckhardt M, Gagen K, et al. Effects of pioglitazone on adipose tissue remodeling within the setting of obesity and insulin resistance. *Diabetes* 2001;50:1863-1871.
18. Fukui Y, Masui S, Osada S, Umesono K, Motojima K. A new thiazolidinedione, NC-2100, which is a weak PPAR-gamma activator, exhibits potent antidiabetic effects and induces uncoupling protein 1 in white adipose tissue of KKAy obese mice. *Diabetes* 2000;49:759-767.
19. Wilson-Fritch L, Nicoloro S, Chouinard M, et al. Mitochondrial remodeling in adipose tissue associated with obesity and treatment with rosiglitazone. *J Clin Invest* 2004;114:1281-1289.
20. Rong JX, Qiu Y, Hansen MK, et al. Adipose mitochondrial biogenesis is suppressed in db/db and high-fat diet-fed mice and improved by rosiglitazone. *Diabetes* 2007;56:1751-1760.
21. Petrovic N, Walden TB, Shabalina IG, Timmons JA, Cannon B, Nedergaard J. Chronic peroxisome proliferator-activated receptor gamma (PPARgamma) activation of epididymally derived white adipocyte cultures reveals a population of thermogenically competent, UCP1-containing adipocytes molecularly distinct from classic brown adipocytes. *J Biol Chem* 2010;285:7153-7164.
22. Seale P, Conroe HM, Estall J, et al. Prdm16 determines the thermogenic program of subcutaneous white adipose tissue in mice. *J Clin Invest* 2011;121:96-105.
23. Kajimura S, Seale P, Spiegelman BM. Transcriptional control of brown fat development. *Cell Metab* 2010;11:257-262.
24. Wu J, Cohen P, Spiegelman BM. Adaptive thermogenesis in adipocytes: is beige the new brown? *Genes Dev* 2013;27:234-250.
25. Giralt M, Villarroya F. White, brown, beige/brite: different adipose cells for different functions? *Endocrinology* 2013;154:2992-3000.
26. Kus V, Flachs P, Kuda O, et al. Unmasking differential effects of rosiglitazone and pioglitazone in the combination treatment with n-3 fatty acids in mice fed a high-fat diet. *PLoS One* 2011;6:e27126.
27. Horakova O, Medrikova D, van Schothorst EM, et al. Preservation of metabolic flexibility in skeletal muscle by a combined use of n-3 PUFA and rosiglitazone in dietary obese mice. *PLoS One* 2012;7:e43764.
28. Tai TA, Jennermann C, Brown KK, et al. Activation of the nuclear receptor peroxisome proliferator-activated receptor gamma promotes brown adipocyte differentiation. *J Biol Chem* 1996;271:29909-29914.
29. Foellmi-Adams LA, Wyse BM, Herron D, Nedergaard J, Kletzien RF. Induction of uncoupling protein in brown adipose tissue. synergy between norepinephrine and pioglitazone, an insulin-sensitizing agent. *Biochem Pharmacol* 1996;52:693-701.
30. Kelly LJ, Vicario PP, Thompson GM, et al. Peroxisome proliferator-activated receptors gamma and alpha mediate in vivo regulation of uncoupling protein (UCP-1, UCP-2, UCP-3) gene expression. *Endocrinology* 1998;139:4920-4927.
31. Barbera MJ, Schluter A, Pedraza N, Iglesias R, Villarroya F, Giralt M. Peroxisome proliferator-activated receptor alpha activates transcription of the brown fat uncoupling protein-1 gene. A link between regulation of the thermogenic and lipid oxidation pathways in the brown fat cell. *J Biol Chem* 2001;276:1486-1493.
32. Liang H, Ward WF. PGC-1alpha: a key regulator of energy metabolism. *Adv Physiol Educ* 2006;30:145-151.
33. Rakhshandehroo M, Knoch B, Muller M, Kersten S. Peroxisome proliferator-activated receptor alpha target genes. *PPAR Res* 2010; 612089.
34. Seale P, Kajimura S, Yang W, et al. Transcriptional control of brown fat determination by PRDM16. *Cell Metab* 2007;6:38-54.